SUPPLEMENT ARTICLE

Conserved Proline-Rich Region of Ebola Virus Matrix Protein VP40 Is Essential for Plasma Membrane Targeting and Virus-Like Particle Release

Olivier Reynard,[1] Kirill Nemirov,[1] Audrey Page,[1] Mathieu Mateo,[1] Hervé Raoul,[2] Winfried Weissenhorn,[3] and Viktor E. Volchkov[1]

[1]Filovirus Laboratory, INSERM U758, Human Virology Department, Claude Bernard Université Lyon 1, Ecole Normale Supérieure de Lyon, [2]Laboratoire P4 INSERM Jean Mérieux, Lyon, and [3]Unit of Virus Host Cell Interactions, UMI 3265, Université Joseph Fourier-EMBL-CNRS, Grenoble, France

The matrix protein VP40 is essential for Ebola virus (EBOV) and Marburg virus assembly and budding at the plasma membrane. In this study we have investigated the effect of single amino acid substitutions in a conserved proline-rich region of the EBOV VP40 located in the carboxy-terminal part of the protein. We demonstrate that substitutions within this region result in an alteration of intracellular VP40 localization and also cause a reduction or a complete block of virus-like particle budding, a benchmark of VP40 function. Furthermore, some mutated VP40s revealed an enhanced binding with cellular Sec24C, a part of the coat protein complex II (COPII) vesicular transport system. Analysis of the 3-dimensional structure of VP40 revealed the spatial proximity of the proline-rich region and an earlier identified site of interaction with Sec24C, thus allowing us to hypothesize that the altered intracellular localization of the VP40 mutants is a consequence of defects in their interaction with COPII-mediated vesicular transport.

The Filoviridae family, a group of negative-strand RNA viruses that can cause severe hemorrhagic fever in humans, consists of 2 genera, *Ebolavirus* and the closely related *Marburgvirus* [1]. The genome of *Zaire ebolavirus*, a member of the first genus, is ~19 kb long and contains 7 genes arranged in a linear order [2]. Four structural proteins, nucleoprotein (NP), VP35, VP30, and the RNA-dependent RNA polymerase (L) together with genomic RNA, form the ribonucleoprotein complex and are involved in replication and transcription of viral RNAs [3]. The surface of virus particles is decorated by the single glycoprotein GP, generated through transcriptional RNA editing of the GP gene [4, 5]. Two proteins, VP40 and VP24, are considered to be the matrix proteins [6]. VP24 is a multifunctional protein that is involved in viral nucleocapsid maturation [7], antagonizes interferon signaling [8] and has also been shown to undergo changes during adaptation to new animal hosts [9]. VP40 is the major matrix protein, playing a crucial role in the assembly and budding of virus particles [10–14].

Structurally, Ebola virus (EBOV) VP40 consists of 2 loosely associated domains connected by a flexible linker [15]. The N-terminal domain promotes protein oligomerization, whereas the C-terminal domain is responsible for membrane binding [16]. Deletion of the C-terminal domain prevents both association of VP40 with lipid bilayers and formation of VP40 hexamers [17]. VP40 octamers represent another oligomeric form of this protein, which is formed in a sequence-specific manner and incorporates single-stranded RNA [18, 19].

Potential conflicts of interest: none reported.

Presented in part: Third European Congress of Virology, Nurnberg, Germany, 2007. Abstract NII031.

Correspondence: Viktor E. Volchkov, PhD, Filovirus Laboratory, INSERM U758, ENS Lyon, Claude Bernard University Lyon-1, 21, Ave Tony Garnier 69365, Lyon Cedex 07, France (viktor.volchkov@inserm.fr).

The Journal of Infectious Diseases 2011;204:S884–S891

0022-1899 (print)/1537-6613 (online)/2011/204S3-0019$14.00
DOI: 10.1093/infdis/jir359

The oligomeric forms of VP40 appear to play different roles in the virus life cycle: the hexamers have been implicated in viral morphogenesis and budding, whereas octamers, although essential, are not involved in the budding process [20]. Expression of EBOV VP40 alone leads to formation of filamentous virus-like particles (VLPs) [21, 22], a benchmark of VP40 function. EBOV structural proteins, including VP40, recruit the ESCRT (endosomal sorting complex required for transport) factors to facilitate late steps in budding, including membrane fission (pinching off the vesicles) [23]. Two overlapping late domains are located at the amino terminus of VP40 and recruit the ESCRT-I proteins TSG101 and Nedd4, an E3 ubiquitin ligase, to the site of virus budding at the plasma membrane [24, 25]. Additional putative functions of the C-terminal domain of VP40 in membrane binding have been highlighted in a number of publications [26–28]. Recently, Yamayoshi and coauthors demonstrated that EBOV VP40 interacts with cellular Sec24C, a member of the coat protein complex II (COPII), mediating anterograde transport of proteins from the endoplasmic reticulum to the Golgi apparatus [27].

In the current study, we investigated the role of a conserved proline-rich region of EBOV VP40. We demonstrate that this region is essential for VP40 transport to the plasma membrane. Certain amino acid substitutions in this region lead to an increase in the binding of VP40 with Sec24C. Intriguingly, mapping of the proline-rich region on the 3-dimensional structure of EBOV VP40 [15, 29] revealed the close spatial proximity of the identified region and the proposed Sec24C-binding site (amino acids 303–308).

MATERIALS AND METHODS

Cells, Plasmids, Mutagenesis, Transfections, and Virus

HEK 293T and Vero E6 cells were cultured in Dulbecco's modified Eagle's medium (Invitrogen) supplemented with 10% fetal calf serum at 37°C. The cells were grown for 24 hours to a confluence of ~60%. VP40 from *Zaire ebolavirus*, strain Mayinga, was subcloned from plasmid pcDNA3.1(+) [30] into the vector phCMV [31] using the restriction endonuclease *Eco*RI. The VP40 mutants (P205D, H210E, P211D, K212S, L213S, P215D, L218A, P219D, M305A, and V306A) were created using phCMV-EBOV/VP40 and the QuikChange site-directed mutagenesis kit (Stratagene), according to the supplier's instructions. Plasmids encoding N-terminally myc-tagged wild-type VP40 (wtVP40) and myc-H210E-VP40 were generated by polymerase chain reaction amplification of the VP40 sequences from the corresponding plasmids using primers supplemented with *Eco*RI restriction sites: 5′- AAGAATTC*ATGGAACAAAAA CTCATCTCAGAAGAGGATCTG*TTGAGGCGGGTTATATTG and 5′- TT*GAATTC*TTACTTCTCAATCACAGCTGG. Polymerase chain reaction fragments were introduced into phCMV using a unique restriction site *Eco*RI. Transfection of cells in 6-well plates was performed using Fugene HD (Roche) or Exgen 500 (Euromedex) reagent, according to the manufacturer's instructions. The cells were collected 18–20 hours after transfection if not otherwise indicated. Protein samples were separated by sodium dodecyl sulfate–polyacrylamide gel electrophoresis (SDS-PAGE) and detected by immunoblotting using monoclonal anti–EBOV-VP40 antibodies.

VLP Assay

Culture supernatants from HEK 293T cells transfected with plasmids encoding wtVP40 or mutated VP40s were collected 48 hours after transfection. Cellular debris was removed by centrifugation at 1000 × *g*. Clarified supernatants were loaded onto a 20% sucrose cushion and centrifuged at 250000 × *g* for 2 hours at 4°C. The pellet was resuspended in phosphate-buffered saline and then subjected to Western blot analysis using anti-VP40 antibody 9B12 (EMBL).

Flotation Assay

HEK 293T cells expressing VP40 were resuspended in a hypotonic buffer (10 mmol/L Tris–hydrochloric acid, pH 7.5; 1 mmol/L ethylenediaminetetraacetic acid; 0.25 mol/L sucrose). The cells were lysed with 30 strokes of a Dounce homogenizer and the lysates cleared by centrifugation at 1000 rpm for 5 minutes. Cleared supernatants were adjusted to 40% HistoDenz (weight/weight), loaded at the bottom of a tube, and layered with 30% and 10% HistoDenz. After centrifugation in a Beckman SW41 rotor at 200000 × *g* for 20 hours, the gradient fractions were collected from the bottom to the top and assessed by Western blot analysis using anti-VP40 antibody.

Ultracentrifugation Analysis Using an Isopycnic Iodixanol Gradient

HEK 293T cells were transfected with tetanus neurotoxin-insensitive vesicle-associated membrane protein (TI-VAMP) green fluorescent protein (GFP), cellubrevin-GFP (kind gift of T. Galli), and phCMV-EBOV/VP40 or mutated VP40s. Samples of cells were collected 20 hours after transfection and resuspended in a hypotonic buffer as aforementioned. Cleared by low-speed centrifugation, lysates were divided into 3 parts and adjusted to 10%, 20%, or 30% iodixanol, respectively. Isopycnic gradients were made as described elsewhere [24, 32]. Samples were subjected to ultracentrifugation in a Beckman SW60 rotor at 250000 × *g* for 4 hours. Gradient fractions were collected from the bottom and assessed with Western blot analysis.

Indirect Immunofluorescence and Nocodazole Treatment

Vero E6 cells were transfected with plasmids expressing different VP40 constructs. Sixteen hours after transfection, cells were fixed using a methanol-acetone mix (1:1) or 4% paraformaldehyde followed by 0.1% Triton X100 permeabilization. For nocodazole experiments plasmid transfected cells were washed 4 hours after transfection and then incubated for

15 hours in either the absence or presence of 10 μmol/L nocodazole (Sigma-Aldrich). The cells were fixed as described above. Immunofluorescence analysis was performed using mouse monoclonal anti-VP40 antibody (1:200) or rabbit antitubulin antibody (1:200) and secondary donkey antimouse Alexa 488–coupled antibody (1:2000; Invitrogen) or donkey antirabbit Alexa 555–coupled antibody (1:2000; Invitrogen). Nuclei were stained with 4,6-diamidino-2-phenylindole (Invitrogen). Pictures were taken using a Zeiss Axio M200 or a Leica confocal SP5 microscope. Sec24C was stained using mouse anti-c-myc 9E10 antibody directly coupled to Alexa 555 (Millipore).

Coimmunoprecipitation Assay

HEK 293T cells were transfected with plasmids expressing c-myc–tagged Sec24C and either wtVP40 or mutated VP40s. Samples of cells were collected 20 hours after transfection, lysed and cleared by low-speed centrifugation as aforementioned. Coimmunoprecipitation was performed using anti-c-myc magnetic beads (Miltenyi μMACS c-myc Isolation Kit) in accordance with the manufacturer's recommendations (Miltenyi Biotec).

RESULTS

Comparative sequence analysis of the matrix protein VP40 from several species of EBOV and Marburg virus using AlignX (Invitrogen) identified a conserved proline-rich region of 15 amino acids (amino acids 205–219) located within the carboxy-terminal domain of VP40 (Figure 1*A*). To clarify the role of this conserved region in the function of VP40, a set of plasmids expressing single amino acid VP40 mutants was generated and used for transient expression in Vero E6 cells (Figure 1*B*). First, wtVP40 and the VP40 mutants were assayed for their intracellular localization by immunofluorescence microscopy using anti-VP40 antibodies. Three distinct patterns of VP40 distribution were distinguished (Figure 1*C*). wtVP40, K212S, and L218A revealed an overall cytoplasmic staining, including an intense staining of membrane protrusions formed by VP40-expressing cells. Two other mutants, P211D and P215D, demonstrated diffuse cytoplasmic staining, which was accompanied by the concentration of VP40 in clumplike inclusions close to the plasma membrane. Other VP40 mutants, P205D, H210E, L213S, and P219D (data not shown), revealed massive VP40 inclusions within the perinuclear area with weak diffused cytoplasmic staining. Noticeably, this group of mutants was also characterized by the apparent absence of VP40 at the plasma membrane. The latter observation was confirmed in experiments where the mutants were coexpressed with the amino-terminal part of Vps28 fused with GFP (VPS28N-GFP). ESCRT-I proteins are known to be associated with the endosomal compartment and recently were also shown to be massively present at the plasma membrane [34]. Confocal microscopy analysis demonstrated that wtVP40 is colocalized with VPS28N-GFP at the plasma

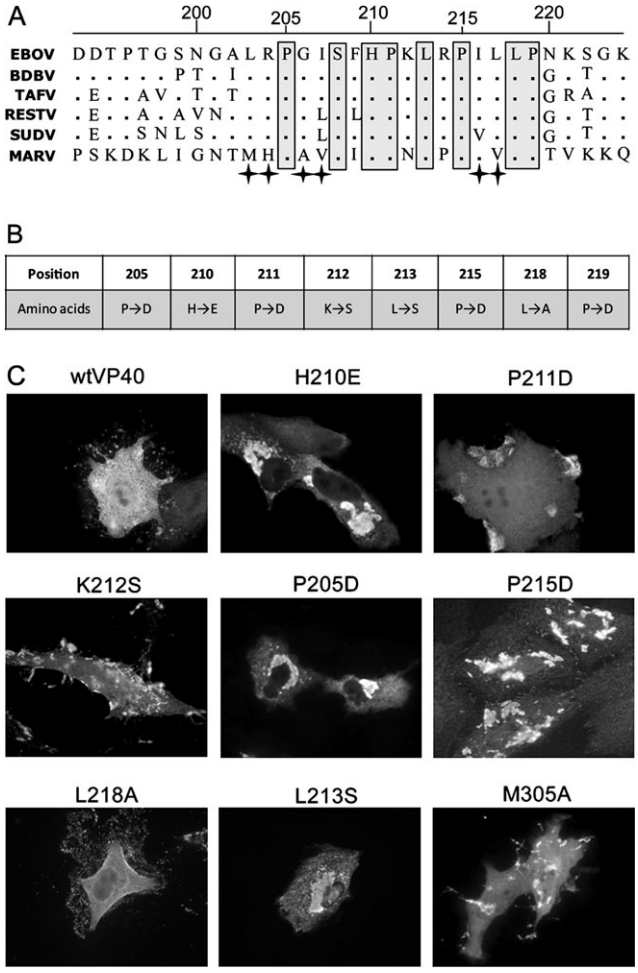

Figure 1. Intracellular localization of Ebola virus (EBOV) VP40 mutants containing amino acid substitutions in the conserved proline-rich region (amino acids 205–219) located at the carboxy-terminal part of the protein. *A,* Partial alignment of filovirus VP40 amino acid sequences. Sequences used for the alignment include EBOV (NC_002549.1), Reston virus (RESTV) (NC_004161.1), Sudan virus (SUDV) (FJ968794.1), Taï Forest virus (TAFV) (FJ217162.1), Bundibugyo virus (BDBV) (FJ217161.1), and Marburg virus (MARV) (Z12132.1). Amino acids identical between all sequences are outlined (*gray boxes*), and conservative amino acids [33] are marked by asterisks. *B,* Set of amino acid substitutions in EBOV VP40. *C,* Immunofluorescence analysis of Vero E6 cells expressing different VP40 mutants. Three fluorescent patterns are illustrated; wtVP40, wild-type VP40. M305A-VP40 was shown elsewhere to possess increased binding to Sec24C [27].

membrane and also in cellular protrusions. In contrast, plasma membranes of H210E-expressing cells were stained exclusively by VPS28N-GFP (Figure 2*A*) [34].

After showing that mutations in the proline-rich region differentially affect VP40 intracellular distribution, we investigated whether these mutations altered the release of VLPs. Thus, we chose 3 VP40s: wtVP40, H210E-VP40 and P211D-VP40 which represented 3 distinct patterns of the protein's intracellular localization. As shown in Figure 2*B*, expression of wtVP40 led to

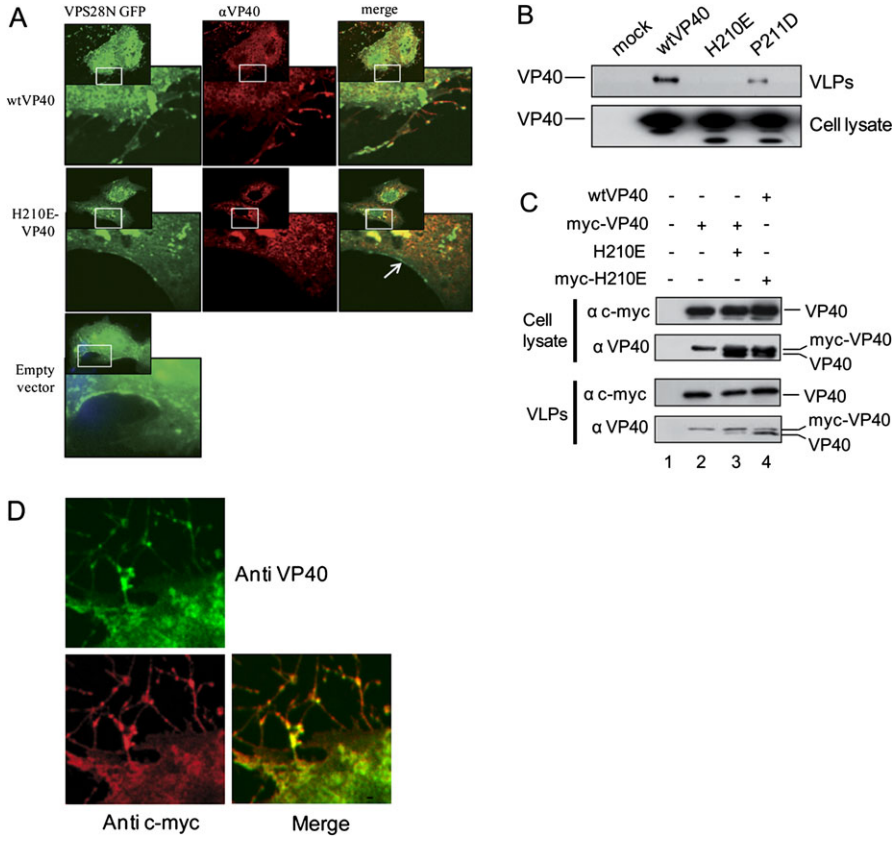

Figure 2. *A,* Plasma membrane association, showing coexpression of empty vector, wild-type VP40 (wtVP40), or H210E-VP40 (*red*) with the N-terminal domain of VPS28 fused to green fluorescent protein (GFP) (VPS28N-GFP) (*green*). Areas present within the frame are displayed as enlarged pictures. *B,* Release of virus-like particles (VLPs). HEK 293T cells were transfected with plasmids expressing either wtVP40 or mutated H210E-VP40 and P211D-VP40, and VLPs from culture supernatants and cell lysates were assessed with Western blot analysis. *C,* Recovery of VLP release; wtVP40 and mutated H210E-VP40 were coexpressed in HEK 293T cells. Cell lysates and VLPs from culture supernatants were subjected to Western blot analysis, using anti–c-myc and anti-VP40 antibodies, as indicated. Mock-transfected cells were loaded in lane 1. *D,* Recovery of membrane association. Confocal microscopy of HEK 293T cells coexpressing wtVP40 (*green*) and c-myc–tagged H210E-VP40 (*red*).

the release of VLPs whereas significantly fewer VLPs were found in the culture medium of P211D-VP40–expressing cells, and a complete block in VLP release was seen with H210E-VP40.

Release of VLPs is known to be associated with VP40 oligomerization, which is induced by interaction with lipid membranes [18–20]. To determine whether the substitutions in the proline-rich domain altered VP40 functional oligomerization, mutants defective in VLP release were coexpressed with wtVP40. We supposed that both proteins would be included in VLPs if the oligomerization pattern were not altered by mutations, and, vice versa, that the VLPs would exclusively contain wtVP40 if the oligomerization were affected by mutations. To distinguish wild-type and mutated proteins, plasmids expressing c-myc–tagged VP40s were constructed. Notably, addition of the myc-tag resulted in a shift in protein migration during SDS-PAGE. As shown in Figure 2*C*, coexpression of c-myc–tagged wtVP40 with the nontagged H210E-VP40, or nontagged wtVP40 with the myc-tagged H210E-VP40 resulted in recovery of H210E-VP40's ability to form VLPs. Confocal microscopy analysis confirmed the plasma membrane localization of c-myc–tagged H210E in the wtVP40-expressing cells (Figure 2*D*).

Because mutant H210E-VP40 appears to be absent from the plasma membrane, we investigated whether substitutions in the proline-rich domain alter the ability of VP40 to interact with lipid membranes. wtVP40 and H210E-VP40 were expressed in HEK293T cells and then analyzed using a flotation assay (Figure 3*A*). Both wtVP40 and H210E-VP40 were found at the top of the gradient, in fractions representing floating lipid membranes. To further investigate whether the proteins nonetheless differ in their association with specific membrane compartments, the cell samples expressing either wtVP40 or H210E-VP40 were separated by isopycnic centrifugation in iodixanol gradients. TI-VAMP–GFP, cellubrevin-GFP (late endosome and plasma membrane) [35], and Lamp1 were used as markers of different intracellular compartments. Remarkably, H210E-VP40 was absent in fractions containing the plasma membrane but was present in fractions containing other membrane compartments. In contrast, wtVP40 was found in all

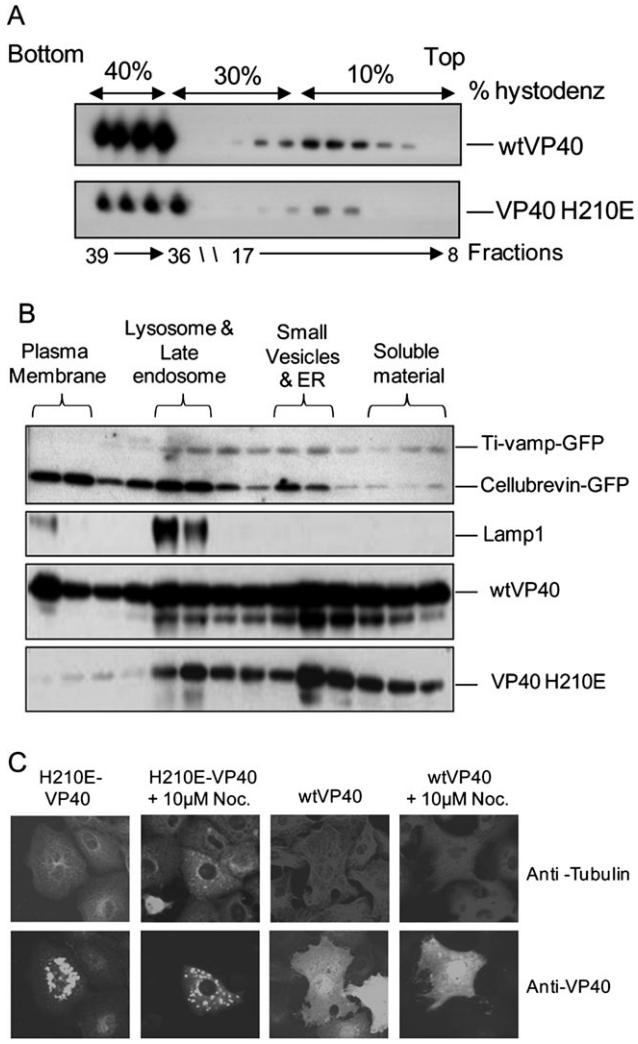

Figure 3. Membrane association of Ebola virus (EBOV) VP40. *A,* Flotation assay using a HistoDenz gradient. HEK 293T cells were transfected with phCMV-EBOV/VP40 or phCMV-EBOV/H210E-VP40, and cell lysates were analyzed by centrifugation using a discontinuous HistoDenz gradient (40%, 30%, 10%). Gradient fractions are indicated; wtVP40, wild-type VP40. *B,* Flotation assay using isopycnic gradient. HEK 293T cells were transfected with plasmids as aforementioned and plasmids expressing markers tetanus neurotoxin-insensitive vesicle-associated membrane protein (TI-VAMP)–green fluorescent protein (GFP) and cellubrevin-GFP for particular cellular membrane compartments. Gradient fractions were harvested from the bottom to the top. Fractions were assessed by 10% sodium dodecyl sulfate–polyacrylamide gel electrophoresis and subsequent Western blot analysis using Lamp1-, GFP- and VP40-specific antibodies. Fractions containing different membrane compartments are indicated. *C,* Effect of nocodazole (Noc.) treatment on intracellular distribution of VP40. HEK 293T cells expressing either wtVP40 or H210-VP40 were treated with 10 μmol/L nocodazole or left untreated. Upper panel shows staining with antitubulin antibody; lower panel, staining with anti-VP40 antibody; ER, endoplasmic reticulum.

fractions containing lipid membranes including the plasma membrane (Figure 3*B*). Taken together, the results presented so far suggest that absence of mutated VP40 at the plasma membrane could be due to an alteration in the protein's intracellular trafficking rather than in oligomerization or membrane binding.

It has been demonstrated elsewhere that VP40 interacts with cellular tubulin, suggesting that the microtubule network is used for the protein's intracellular transport [26]. In this study, we evaluated the impact of the tubulin depolymerizing agent nocodazole on the intracellular distribution of wtVP40 and H210E-VP40. Because wtVP40 facilitates tubulin polymerization by stabilizing VP40-associated microtubules, nocodazole treatment did not noticeably alter the distribution of wtVP40 in the cells (Figure 3*C*). Interestingly, formation of perinuclear inclusions by H210E-VP40 was visibly affected by the treatment. Under the treatment, cells expressing H210E-VP40 showed a punctuate fluorescence pattern (Figure 3*C*), indicating that H210E-VP40 aggregates are initially formed outside the perinuclear area.

Recently, Yamayoshi and coauthors have shown that Sec24C, a member of the COPII vesicular transport system, is crucial for VP40 transport and for budding of VLPs [27]. Intriguingly, mapping of the proline-rich region on the 3-dimensional structure of EBOV VP40 [15, 29] revealed the spatial proximity (Figure 4*A*) of the identified proline-rich region (amino acids 205–219) and the proposed Sec24C-binding site (amino acids 303–308). It was thus of interest to investigate whether substitutions in the proline-rich region could affect the interaction of VP40 with Sec24C. wtVP40, H210E-VP40, and P211D-VP40 along with mutated VP40s shown elsewhere to possess increased (M305A) or decreased (V306A) Sec24C binding were co-expressed with c-myc–tagged Sec24C in HEK 293T cells and then assayed by coimmunoprecipitation. Remarkably, in comparison with wtVP40, H210E-VP40 showed a significant increase in binding with Sec24C. Mutant P211D also demonstrated an increase in Sec24C binding in comparison with the wtVP40 but appeared to be less efficient than H210E-VP40. As expected, mutant M305A, described elsewhere by Yamayoshi and coauthors [27], demonstrated an increased binding with Sec24C, whereas mutant V306A was defective in Sec24C binding (Figure 4*B*).

DISCUSSION

The matrix protein VP40 of EBOV is responsible for virus budding and when expressed in a mammalian cell without other viral proteins facilitates the release of VLPs [15, 26, 29, 36]. Here, we investigated the role of a proline-rich region conserved among filoviruses (amino acids 205–219) located in the carboxy-terminal part of VP40. We have demonstrated that single amino acid substitutions in this region result in an alteration of the intracellular distribution of VP40 and an accumulation of mutated VP40s, either in the perinuclear area or in clumps at the plasma membrane. Remarkably, a dramatic reduction in the release of the VLPs was observed with the

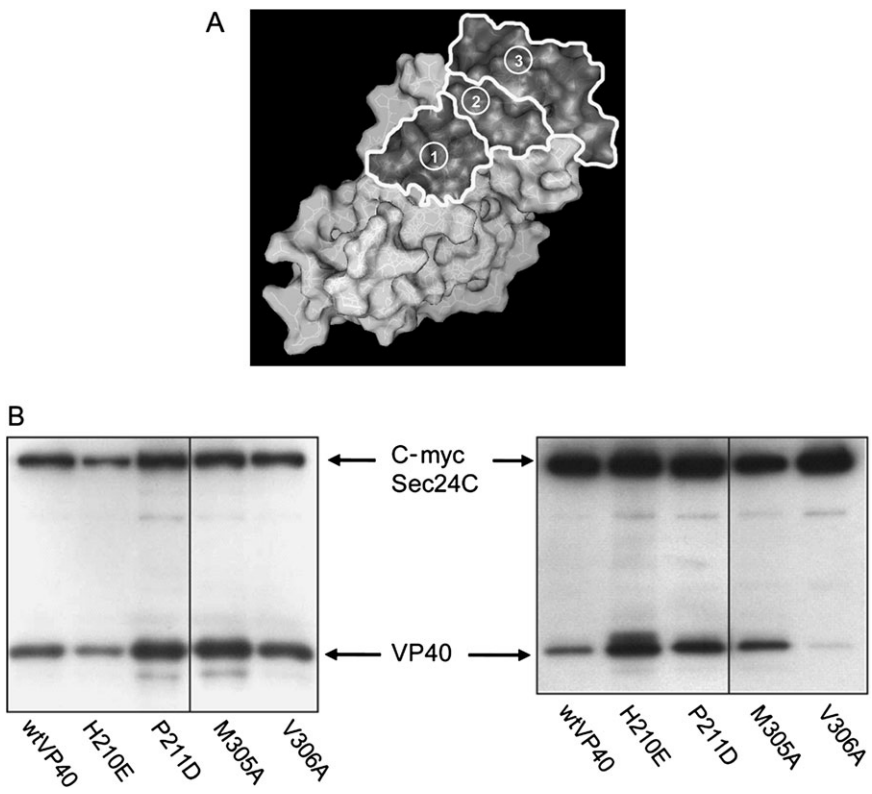

Figure 4. EBOV) VP40 interacts with cellular Sec24C. *A,* Schematic representation of the surface localization of VP40 regions, showing 3-dimensional structure of VP40 [15]; protein data bank identifier, 1ES6). Three EBOV VP40 regions are indicated: amino acids 205–219 (1), 303–308 (2), and 223–253. *B,* Coimmunoprecipitation analysis. HEK 293T cells were transfected with plasmids expressing different VP40 mutants, as indicated, and a plasmid expressing c-myc–tagged Sec24C; wtVP40, wild-type VP40. Left panel, Samples of cells were assessed by sodium dodecyl sulfate–polyacrylamide gel electrophoresis or Western blot analysis before immunoprecipitation. Right panel, Samples of cells were assessed by immunoprecipitation (c-myc–tagged Sec24C), followed by Western blot analysis using anti-VP40 antibodies. Coimmunoprecipitated VP40s are indicated.

majority of the VP40 mutants. It should be mentioned that the lysine residue at position 212 and the surrounding region has attracted significant attention from researchers in the past. Ruigrok et al demonstrated that trypsin proteolysis of full-length VP40 results in cleavage of the protein after lysine 212 and spontaneous dissociation of the C-terminal part of the protein, underlining its weak interaction with the N-terminal part [16].

Furthermore, these authors also showed that removal of this C-terminal part induces the hexamerization of VP40 in vitro, suggesting that the C-terminal domain may sterically prevent protein oligomerization. Scianimanico et al, investigating the role of the carboxy-terminal part of VP40, demonstrated that membrane-association of monomeric VP40 is a starting point in protein oligomerization [17]. Dessen et al elucidated the crystal structure of VP40 and suggested that the region located between β strands 7 and 8 in the C-terminal domain may provide certain flexibility with respect to the N-terminal domain, which might be necessary for the conformational changes required during protein oligomerization or for accommodation of other functions attributed to VP40 during the virus life cycle [15]. The involvement of amino acids 212KLR214 in the release of VLPs was further addressed by McCarthy et al [28]. In the model proposed by these authors, defects in VLP release caused by substitutions of these 3 residues were explained by improper VP40 oligomerization and formation of an unordered VP40 lattice at the plasma membrane, insufficient for the induction of VLP budding [28].

The data obtained in our study highlight an alternative function of the proline-rich region in VLP release. In effect, we demonstrate that the majority of our VP40 mutants, in particular those forming inclusions at the perinuclear area, are not present at the plasma membrane. This observation itself could adequately explain the defect in the release of VLPs. However, we also demonstrate that coexpression of mutants and wtVP40 restores an appearance of mutated proteins at the plasma membrane and facilitates the release of VLPs containing mutated VP40. These results suggest that the proline-rich region could have other functions in addition to the proposed participation in VP40 oligomerization.

Membrane association of VP40 is key to virus assembly because it induces conformational changes required for the protein's oligomerization [17]. It is believed that during trafficking to the plasma membrane, VP40 is associated with different cellular membrane compartments [32, 37]. Using 2 flotation

assays, we have demonstrated that, in contrast to wtVP40, the mutant forming the perinuclear inclusions (H210E-VP40) was not present in fractions containing plasma membranes but targeted other cellular membrane compartments similarly to wtVP40. These results suggest that the substitutions in the proline-rich region of VP40 did not prevent the protein's membrane association but affected intracellular trafficking, thus preventing mutated VP40s from appearing at the plasma membrane.

Several studies have suggested that host cytoskeletal proteins (eg, actin and microtubules) associate with EBOV VP40 and may be important in protein intracellular trafficking [26, 38]. VP40 of EBOV is known to colocalize with microtubule bundles and facilitate tubulin polymerization by stabilizing VP40-associated microtubules [26]. In an attempt to shed light on the mechanism by which VP40 traverses through the cell on the way to the plasma membrane, we evaluated the impact of the tubulin depolymerizing agent nocodazole on the intracellular distribution of VP40. We showed that wtVP40, as expected, was not sensitive to nocodazole treatment. Interestingly, after treatment with nocodazole, instead of aggregates in the perinuclear area, a punctate fluorescence pattern was observed in cells expressing H210E-VP40. The relocalization of H210E-VP40 suggests that the aggregated VP40 lost its ability to stabilize microtubules and in the absence of nocodazole was delivered to the perinuclear area. We speculate that with this treatment the initial sites of H210E-VP40 aggregation become visible. To a certain degree, the pattern of staining and intracellular distribution of such aggregates resembles the staining of the cellular endosomal-lysosomal compartment. Our hypothesis supports the notion that substitutions in the proline-rich region of VP40 affect intracellular VP40 trafficking and is consistent with the function of cellular aggresome–like inclusion bodies that are dependent on retrograde microtubule-based transport [39].

It has recently been demonstrated that EBOV VP40 binds Sec24C, a component of COPII [27]. Yamayoshi et al have proposed that interaction with endoplasmic reticulum–associated Sec24C may initiate intracellular VP40 trafficking via the COPII vesicular transport machinery. Importantly, some mutations in the domain proposed to be a Sec24C binding site (amino acids 303–307) resulted in an alteration in the protein's intracellular distribution and inhibition of VLP budding which were explained by enhanced VP40 binding with Sec24C [27]. Interestingly, our VP40 mutants, including those aggregating within the perinuclear area and those forming clumps at the plasma membrane, also showed a much stronger binding to Sec24C than wtVP40. Intriguingly, the structure of VP40 reveals that the proline-rich region is located in close proximity to the Sec24C binding site (Figure 4*A*). Such a spatial arrangement and also our biochemical analysis data suggest that these 2 regions provide a common platform for VP40 binding with Sec24C. It is noteworthy that at the protein surface these 2 regions are also associated with the region (amino acids 223–253) previously shown to share homology with the tubulin-binding motif found in microtubule-associated protein 2 (Figure 4*A*). The deletion of this region has been shown to result in a loss of VP40 association with the plasma membrane [26], again resembling the appearance of some of our VP40 mutants. Because the COPII transport complex [26, 40, 41] and also EBOV VP40 are associated with microtubules, the spatial arrangement of all 3 domains in close proximity may have significance in VP40 function. However, further studies are necessary to confirm this hypothesis.

Budding of EBOV and the release of VLPs require the recruitment of components from the cellular complex termed ESCRT-I to the plasma membrane, away from their normal site of function in endosomes [24, 42]. It seems reasonable to assume that an easy dissociation of VP40 from the COPII complex is required. Based on our results, we speculate that VP40 mutants with enhanced binding to Sec24C are defective in VLP release, owing to their inability to dissociate from the complex with Sec24C. In this regard, the VP40 inclusions are likely to be composed of mutated VP40s bound to Sec24C and other proteins of the COPII complex.

In conclusion, our findings indicate that the conserved proline-rich region of VP40 (amino acids 205–219) is part of a domain responsible for interaction with cellular Sec24C. They also emphasize the importance of the dissociation of VP40 from a complex with Sec24C for protein transport to the plasma membrane and subsequent VLP budding. In the future, it will be of interest to further define the role of this region. This will provide insights into the mechanism of VP40 intracellular trafficking and elucidate the molecular details of viral morphogenesis.

Funding

This work was supported by INSERM, Ministère Français de la Recherche (grant 04G537), Agence Nationale de la Recherche (grant ANR-07-MIME-006-01), Fondation pour la Recherche Médicale en France (grant FRM DMI20091117323), and Deutsche Forschungsgemeinschaft (grant SFB 593 to V. E. V.).

Acknowledgments

We thank Yoshi Kawaoka for providing the plasmid expressing c-myc–tagged Sec24C and Thierry Galli for cellubrevin-GFP and TI-VAMP–GFP. We are also grateful to Robin Buckland for helpful comments on the manuscript.

References

1. Peters CJ, LeDuc JW. An introduction to Ebola: the virus and the disease. J Infect Dis **1999**; 179(Suppl 1):ix–xvi.
2. Sanchez A, Kiley MP, Holloway BP, Auperin DD. Sequence analysis of the Ebola virus genome: organization, genetic elements, and comparison with the genome of Marburg virus. Virus Res **1993**; 29:215–40.
3. Muhlberger E, Weik M, Volchkov VE, Klenk HD, Becker S. Comparison of the transcription and replication strategies of Marburg virus

and Ebola virus by using artificial replication systems. J Virol **1999**; 73:2333–42.
4. Volchkov VE, Becker S, Volchkova VA, et al. GP mRNA of Ebola virus is edited by the Ebola virus polymerase and by T7 and vaccinia virus polymerases. Virology **1995**; 214:421–30.
5. Volchkov VE, Volchkova VA, Muhlberger E, et al. Recovery of infectious Ebola virus from complementary DNA: RNA editing of the GP gene and viral cytotoxicity. Science **2001**; 291:1965–9.
6. Feldmann H, Klenk HD, Sanchez A. Molecular biology and evolution of filoviruses. Arch Virol Suppl **1993**; 7:81–100.
7. Noda T, Halfmann P, Sagara H, Kawaoka Y. Regions in Ebola virus VP24 that are important for nucleocapsid formation. J Infect Dis **2007**; 196(Suppl 2):S247–50.
8. Reid SP, Leung LW, Hartman AL, et al. Ebola virus VP24 binds karyopherin alpha1 and blocks STAT1 nuclear accumulation. J Virol **2006**; 80:5156–67.
9. Volchkov VE, Chepurnov AA, Volchkova VA, Ternovoj VA, Klenk HD. Molecular characterization of guinea pig-adapted variants of Ebola virus. Virology **2000**; 277:147–55.
10. Byland R, Marsh M. Trafficking of viral membrane proteins. Curr Top Microbiol Immunol **2005**; 285:219–54.
11. Gomis-Ruth FX, Dessen A, Timmins J, et al. The matrix protein VP40 from Ebola virus octamerizes into pore-like structures with specific RNA binding properties. Structure **2003**; 11:423–33.
12. Johnson RF, Bell P, Harty RN. Effect of Ebola virus proteins GP, NP and VP35 on VP40 VLP morphology. Virol J **2006**; 3:31.
13. Johnson RF, McCarthy SE, Godlewski PJ, Harty RN. Ebola virus VP35-VP40 interaction is sufficient for packaging 3E-5E minigenome RNA into virus-like particles. J Virol **2006**; 80:5135–44.
14. Hartlieb B, Weissenhorn W. Filovirus assembly and budding. Virology **2006**; 344:64–70.
15. Dessen A, Volchkov V, Dolnik O, Klenk HD, Weissenhorn W. Crystal structure of the matrix protein VP40 from Ebola virus. EMBO J **2000**; 19:4228–36.
16. Ruigrok RW, Schoehn G, Dessen A, et al. Structural characterization and membrane binding properties of the matrix protein VP40 of Ebola virus. J Mol Biol **2000**; 300:103–12.
17. Scianimanico S, Schoehn G, Timmins J, Ruigrok RH, Klenk HD, Weissenhorn W. Membrane association induces a conformational change in the Ebola virus matrix protein. EMBO J **2000**; 19:6732–41.
18. Hoenen T, Volchkov V, Kolesnikova L, et al. VP40 octamers are essential for Ebola virus replication. J Virol **2005**; 79:1898–905.
19. Timmins J, Schoehn G, Kohlhaas C, Klenk HD, Ruigrok RW, Weissenhorn W. Oligomerization and polymerization of the filovirus matrix protein VP40. Virology **2003**; 312:359–68.
20. Hoenen T, Biedenkopf N, Zielecki F, et al. Oligomerization of Ebola virus VP40 is essential for particle morphogenesis and regulation of viral transcription. J Virol **2010**; 84:7053–63.
21. Timmins J, Scianimanico S, Schoehn G, Weissenhorn W. Vesicular release of Ebola virus matrix protein VP40. Virology **2001**; 283:1–6.
22. Noda T, Sagara H, Suzuki E, Takada A, Kida H, Kawaoka Y. Ebola virus VP40 drives the formation of virus-like filamentous particles along with GP. J Virol **2002**; 76:4855–65.
23. Peel S, Macheboeuf P, Martinelli N, Weissenhorn W. Divergent pathways lead to ESCRT-III-catalyzed membrane fission. Trends Biochem Sci **2011**; 36:199–210.
24. Timmins J, Schoehn G, Ricard-Blum S, et al. Ebola virus matrix protein VP40 interaction with human cellular factors Tsg101 and Nedd4. J Mol Biol **2003**; 326:493–502.
25. Martin-Serrano J, Zang T, Bieniasz PD. HIV-1 and Ebola virus encode small peptide motifs that recruit Tsg101 to sites of particle assembly to facilitate egress. Nat Med **2001**; 7:1313–9.
26. Ruthel G, Demmin GL, Kallstrom G, et al. Association of Ebola virus matrix protein VP40 with microtubules. J Virol **2005**; 79:4709–19.
27. Yamayoshi S, Noda T, Ebihara H, et al. Ebola virus matrix protein VP40 uses the COPII transport system for its intracellular transport. Cell Host Microbe **2008**; 3:168–77.
28. McCarthy SE, Johnson RF, Zhang YA, Sunyer JO, Harty RN. Role for amino acids 212KLR214 of Ebola virus VP40 in assembly and budding. J Virol **2007**; 81:11452–60.
29. Dessen A, Forest E, Volchkov V, Dolnik O, Klenk HD, Weissenhorn W. Crystallization and preliminary X-ray analysis of the matrix protein from Ebola virus. Acta Crystallogr D Biol Crystallogr **2000**; 56:758–60.
30. Basler CF, Wang X, Muhlberger E, et al. The Ebola virus VP35 protein functions as a type I IFN antagonist. Proc Natl Acad Sci U S A **2000**; 97:12289–94.
31. Yee JK, Miyanohara A, LaPorte P, Bouic K, Burns JC, Friedmann T. A general method for the generation of high-titer, pantropic retroviral vectors: highly efficient infection of primary hepatocytes. Proc Natl Acad Sci U S A **1994**; 91:9564–8.
32. Kolesnikova L, Bamberg S, Berghofer B, Becker S. The matrix protein of Marburg virus is transported to the plasma membrane along cellular membranes: exploiting the retrograde late endosomal pathway. J Virol **2004**; 78:2382–93.
33. Dagan T, Talmor Y, Graur D. Ratios of radical to conservative amino acid replacement are affected by mutational and compositional factors and may not be indicative of positive Darwinian selection. Mol Biol Evol **2002**; 19:1022–5.
34. Welsch S, Habermann A, Jager S, Muller B, Krijnse-Locker J, Krausslich HG. Ultrastructural analysis of ESCRT proteins suggests a role for endosome-associated tubular-vesicular membranes in ESCRT function. Traffic **2006**; 7:1551–66.
35. Grigorov B, Arcanger F, Roingeard P, Darlix JL, Muriaux D. Assembly of infectious HIV-1 in human epithelial and T-lymphoblastic cell lines. J Mol Biol **2006**; 359:848–62.
36. Panchal RG, Ruthel G, Kenny TA, et al. In vivo oligomerization and raft localization of Ebola virus protein VP40 during vesicular budding. Proc Natl Acad Sci U S A **2003**; 100:15936–41.
37. Kolesnikova L, Bugany H, Klenk HD, Becker S. VP40, the matrix protein of Marburg virus, is associated with membranes of the late endosomal compartment. J Virol **2002**; 76:1825–38.
38. Han Z, Harty RN. Packaging of actin into Ebola virus VLPs. Virol J **2005**; 2:92.
39. Kopito RR. Aggresomes, inclusion bodies and protein aggregation. Trends Cell Biol **2000**; 10:524–30.
40. Presley JF, Cole NB, Schroer TA, Hirschberg K, Zaal KJ, Lippincott-Schwartz J. ER-to-Golgi transport visualized in living cells. Nature **1997**; 389:81–5.
41. Noda T, Ebihara H, Muramoto Y, et al. Assembly and budding of Ebolavirus. PLoS Pathog **2006**; 2:e99.
42. Silvestri LS, Ruthel G, Kallstrom G, et al. Involvement of vacuolar protein sorting pathway in Ebola virus release independent of TSG101 interaction. J Infect Dis **2007**; 196(Suppl 2):S264–70.